http:// ijp.mums.ac.ir
Original Article (Pages: 13213-13224)

Formulation, Optimization and Evaluation of Nanofiber Based Fast Dissolving Drug Delivery System of Colchicine for Pediatrics

Hamed Morad [1, 2], *Mohsen Jahanshahi[3], Jafar Akbari[1], Majid Saeedi[1], Pooria Gill[4], *Reza Enayatifard[1]

[1]Department of Pharmaceutics, Faculty of Pharmacy, Mazandaran University of Medical Sciences, Sari, Iran.
[2] Student Research Committee, Mazandaran University of Medical Sciences, Sari, Iran.
[3]Nanotechnology Research Institute, Faculty of Chemical Engineering Babol Noushirvani University of Technology, Babol, Iran.
[4]Department of Medical Nanotechnology, Faculty of Advanced Technologies in Medicine, Mazandaran University of Medical Sciences, Sari, Iran.

Abstract

Systemic toxicity is an obstacle against the oral administration of colchicine. The high body surface area to mass ratio in pediatrics would dramatically enhance the toxicity risk. This issue could be jettisoned by formulation of an optimized nanofiber-based fast dissolving delivery system. It could enhance the drug's bioavailability, reduce the administered dose, and bring more convenience and compliance for pediatrics with the problem of consuming conventional dosage forms. The optimized colchicine loaded nanofibers of polyvinyl alcohol 10%w/v with 220.47±16.87 nm mean diameter size exhibits smooth surface and continuous structure in SEM micrographs. No incompatibility was seen in FT-IR analyses. The thermal study illustrated stability enhancement by colchicine loading. The water angle analysis demonstrated its superhydrophilicity and the in vitro release profile illustrated a quick release of colchicine in 30 seconds. As a conclusion, nanofiber-based fast dissolving formulation of colchicine could be suggested as a localized and systemic transmucosal delivery system, immediate-release oral dosage form, and even topical colchicine delivery system that may reduce the risk of systemic toxicity in pediatrics. The antitumor property of CL may also suggest it in rapid neoadjuvant or adjuvant localized chemotherapy protocols for the management of topical tumors in pediatrics.

Key Words: Colchicine, Fast dissolving drug delivery system, Pediatrics, Nanofiber, Bioavailability.

*Please cite this article as: Morad H, Jahanshahi M, Akbari J, Saeedi M, Gill P, Enayatifard R. Formulation, Optimization and Evaluation of Nanofiber Based Fast Dissolving Drug Delivery System of Colchicine for Pediatrics. Int J Pediatr 2021; 9(3): 13213-224. DOI: **10.22038/IJP.2020.52106.4140**

Corresponding Author:

Mohsen Jahanshahi, Nanotechnology Research Institute, Faculty of Chemical Engineering Babol Noushirvani University of Technology, Babol, Iran.

Reza Enayatifard, Department of Pharmaceutics, Faculty of Pharmacy, Mazandaran University of Medical Sciences, Sari, Iran. Postal code: 4847193698.

Emails: mjahan@nit.ac.ir AND enayatifard_r@yahoo.com

Received date: Dec.20, 2020; Accepted date: Feb. 12, 2021

1- INTRODUCTION

Fast dissolving drug delivery systems have been under the spotlight in last decade. The significant bioavailability enhancement and patient's convenience and compliance are the main advantages of the fast dissolving drug delivery systems (1). The pediatrics with dysphagia, movement problems, mental disorders (2) or those who are on liquid-intake limitation regimen (3) could not easily consume conventional dosage forms. Polyvinyl alcohol (PVA) as a biodegradable and biocompatible polymer possesses a great hydrophilic property which could provide a rapid dissolution rate for drug delivery systems and enhance the bioavailability of loaded drug (4).

Applications of nanofiber-based (NF-based) fabrications in drug delivery are still popular. Nanofibers possess remarkable benefits in comparison with other nanostructures like nanocrystals, liposomes, noisomes, nanofilms, nanotubes, dendrimers, nanospheres, nanorods, solid lipid nanoparticles, nanostructured lipid carriers, etc., which provide great potential for application as effective drug delivery systems. The advantages include large surface area to volume, fine porosity, flexibility, capability of being incorporated with various chemical and biological agents, high encapsulation efficiency, release control, nanoscale diameter size, etc. These unique properties could allow easy penetration of water molecules into the mat and causes fast wetting and dissolution which provides immediate release profiles of loaded agents (5–8).

Colchicine (CL), has various indications in systemic and topical disorders. The systemic indications include hyperuricemia, familial Mediterranean fever, and amyloidosis. Also, more indications were reported in cardiology, oncology, immunology and dermatology. The dermatological diseases include Recurrent aphthous stomatitis, Nodular vasculitis, Urticarial vasculitis, Behcet's disease, Epidermolysis bullosa acquisita, Granuloma annulare, Purpura annularis, Henoch–Schonlein purpura, Neutrophilic urticarial, telangiectoides, Pyoderma gangrenosum, Scleredema, Relapsing polychondritis, Scleredema diabeticorum, Sweet syndrome, Actinic keratosis, and Chronic urticarial (5, 8, 9). The main limited factor that restricts the administration of CL, especially in children, is the reported dose dependent toxicity and the narrow therapeutic index. The high body surface area and low weight in pediatrics would seriously increase the toxicity risk. Therefore, finding a suitable way to improve the bioavailability and reduce the administration dose is crucial and could provide a safe prescription for pediatrics (5, 8, 10)

It is proved by latest studies that optimized and continuous NFs with the thinnest diameter size could provide the highest physicochemical efficiency. The characteristics improvement of NFs could lead to reactivity enhancement of NFs with the environment and may increase its solubility and release rate consequently (10). Therefore, the main aim of the present study is to formulate, optimize and characterize PVA NFs loaded with CL as a fast dissolving drug delivery system to enhance bioavailability, reduce administration dose of CL and also bring more convenience and compliance for pediatric patients.

2- MATERIALS AND METHODS

2-1. Materials

Poly vinyl alcohol (PVA) with 27000 molecular weight was bought from Merck (Germany). CL (HPLC grade) was purchased from Sigma–Aldrich Co. (St. Louis, MO, USA). Ultra-pure water was utilized in all the procedures. All the solvents and reagents applied had

analytical grade in accordance with United States' pharmacopoeia standards.

2-2. Methods

2-2-1. Optimization process of PVA NFs as drug delivery system

The electrospinning apparatus (PN 04, Pars Nano Ris Co., Iran) contains a 5ml syringe which the measured inner diameter size was 140 mm. The rotating collector was covered by aluminum foil. The flow rate was 0.2 ml/h and the electrospinning chamber had 50% humidity condition and 25 ℃ temperature. The optimization process was followed by employing various voltages (10, 12, 15, 18 and 20 kv), and nozzle to collector length (10, 12, 15, 20 cm) of the apparatus. The considered concentrations of PVA included 8%, 10% and 12% w/v in ultrapure water as the solvent.

The optimization assay was conducted by three steps including optical microscope, atomic force microscopy (AFM), and scanning electron microscope (SEM). The best formulation was selected based on beardlessness under optical microscopy in the first step and then by considering mean diameter size, distribution and surface roughness of the fibers by evaluating AFM and SEM analyzing data. Subsequently, the 20% w/w of CL was dissolved in the achieved optimized concentration of PVA solution and after 8 hours stirring, the solution was electrospinned under the attained optimized condition to formulate CL-loaded PVA NFs.

2-2-2. Optimization Assay by optical microscopy

In the first step, the feasibility of nanofibers and the qualitative evaluation of each formulation were conducted by accurate observation of nanofibers under optical microscopy (Shimadzu, Japan), and seeking for any beads or spindles.

2-2-3. Optimization Assay by Atomic Force Microscopy

The AFM microscope was JPK Instrument's NanoWizard II (Berlin, Germany), and its inverted microscope was OLYMPUS IX51 (USA). The imaging mode was contact mode. The cantilevers were made of silicon (USA), and 6 nm tip radius. The scan rate, set point and spring constant were 1 Hz, 1 V and 75 N m−1, respectively. The frequency resonant was kept between 200 and 400 kHz. The analyzing process on images was performed by JPK Processing Instruments software. The morphology investigation and the topographic data collecting including mean diameter size of NFs, diameter size distribution and surface roughness values were performed by AFM analyzing.

2-2-4. Scanning electron microscopy

The morphology of PVA NFs and CL-loaded PVA NFs was investigated by field emission scanning microscopy (FE-SEM, MIRA3 TESCAN, 3.0 Kv, Czech Republic). The Image J software (1.51 J8, NIH, USA) was utilized for mean diameter size calculations.

2-2-5. FTIR spectroscopy

The FTIR spectra of pure PVA, CL, and CL-loaded PVA NF mats were analyzed at the range of 400-4400 cm^{-1}. The spectrophotometer model was WQF 510A from China with resolution of 2 cm^{-1}.

2-2-6. Thermal study

The simultaneous thermal analyses (BAHR thermoanalysis GmbH STA 503, Hullhorst, Germany) of pure PVA, CL, PVA NFs, and CL-loaded PVA NFs were conducted at the thermal range of 10 ℃ to 700 ℃. The atmosphere was argon with increasing rate of 10 ℃/min.

2-2-7. Water angle measurement

Contact angle measurement (CA-500M, Sharif Solar Co., Iran) of PVA mats and CL-loaded PVA mats was performed by leaving a 5 µl water drop on the mats

surface and the drop shape was recorded by digital camera. Five repetitions were considered for each sample.

2-2-8. In vitro release

CL-NFs mat pieces with 25 mg weight and about 2*2 cm^2 were immersed in 30 ml phosphate buffer (PBS, 7.4) with continuous stirring at 150 rpm at room temperature. At intervals of 30, 60, 120, 240 and 360 seconds, 2 ml samples of the medium were withdrawn filtered and injected to HPLC for CL determination. The sink condition was provided by adding the same volume of fresh PBS to the medium after each sampling.

2-2-9. HPLC analysis

HPLC Knauer (Germany) with Knauer XDB-C18 column (5 µm, 4.6×250 mm) was utilized for quantification of CL contents. The samples concentrations were determined by the described assay method in the monograph of colchicine in USP pharmacopeia. The 55:45 (v/v) ratio of methanol and phosphate buffer (pH 5.5±0.05) was used as mobile phase with the flow rate of 1 ml/min. The CL determination was performed by UV detector at 254 nm. The observed retention time was 7.7 minutes, which was in accordance with the mentioned range in the USP monograph (5.5-9.5 min) (11). The prepared solutions of CL in PBS with known concentrations of 0.02, 0.05, 0.1, 0.2, 1, 2, 20, and 200 PPM were injected to HPLC for drawing the standard curve.

2-2-10. Statistical Analysis

One-way ANOVA plus post-hoc analysis (Tukey) was applied using Statistical Package for the Social Sciences (SPSS) Version 17.0. The considered significance value was under 0.05.

3- RESULTS

4-1. Optimization of PVA NFs

The optical microscope with three magnitudes of 10X, 40X and 100X was utilized for qualitative investigation of the electrospun formulations. The qualified formulations which demonstrated fine nanofibers with no detectable beads and spindles were selected for quantitative evaluation by AFM and SEM. **Figures. 1 and 2** demonstrate the microscopic images of 10% and 20% PVA formulations with three magnitudes under 20cm and 20 kv of apparatus conditions as representatives.

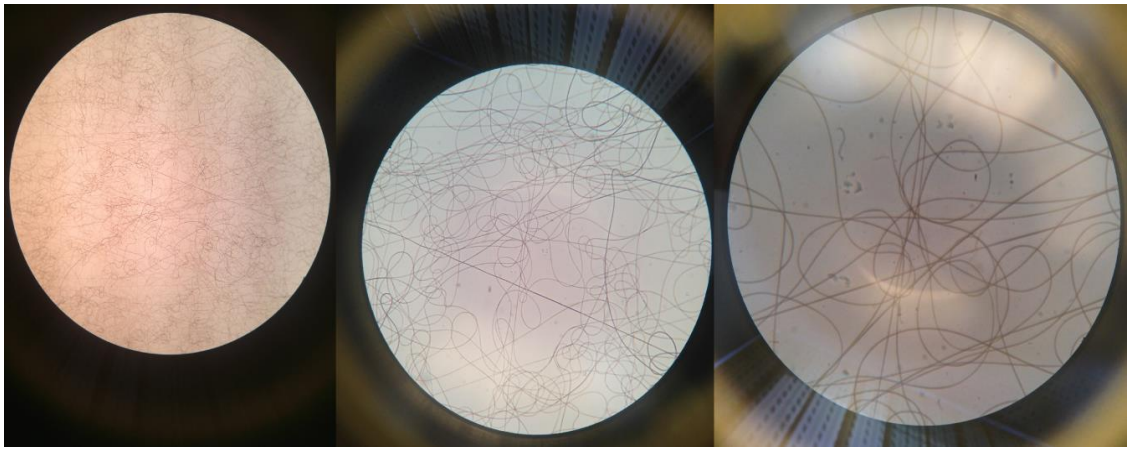

Fig.1: Microscopic images of 10% PVA formulation with 10X, 40X, and 100X magnitudes under 20cm and 20 kv.

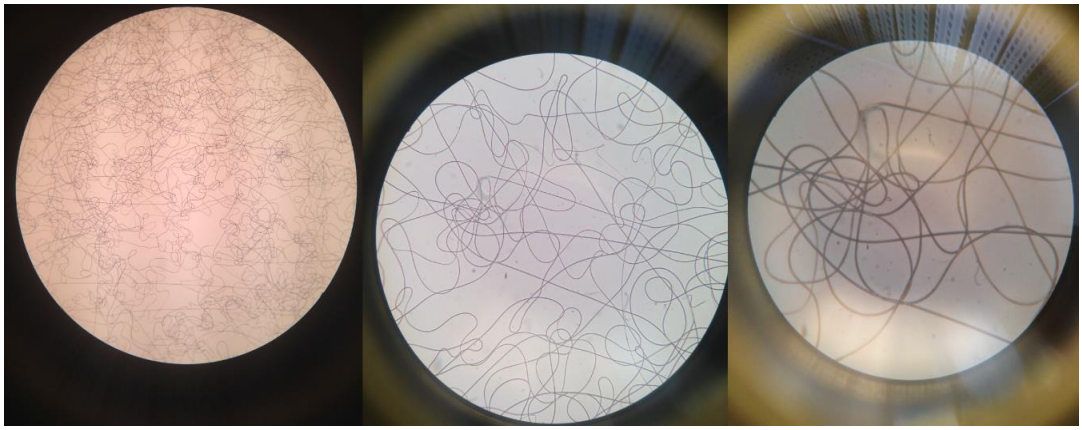

Fig.2: Microscopic images of 12% PVA formulation with 10X, 40X, and 100X magnitudes under 20cm and 20 kv.

The electrospinning results of 8% w/v PVA in all attempted voltages and distances (10cm to 15cm) showed totally bead full NFs but in 20 cm distance at all voltages, almost half of the constructed NFs contained spindles and some beads (**Figures. 3 A and B**). The previous study of Sargazi et al. also reported that non proper formation of NFs could be related to short distance of nozzle-collector that could not provide enough time for solvent evaporation during electrospinning procedure (12). The imperfect production of NFs in 20 cm could be attributed to concentration of the solution. The study of Elkasaby et al. confirmed the key role of polymer concentration on NFs formation and their mean diameter size. Therefore, in next step the 10% w/v and 12% w/v of the PVA were prepared and electrospinned in all mentioned distances and voltages.

The results showed that both concentrations of PVA could produce continuous NFs with high yield.No beads or spindles were detected in the optical microscope andAFM. The achieved optimized parameters for the thinnest NFs were 20 cm distance and 20 kv voltage for both concentrations. (Figures. 3 C and E) (13). The mean diameter size and surface roughness (Sa) for optimized 10% w/v PVA and 12% w/v PVA were 224 nm with 29 nm and 255 nm with 57 nm, respectively. Since the reported mean diameter size, diameter size distribution and surface roughness of 10% PVA were a bit better than 12% PVA, the formulation of 10% PVA with 20cm nozzle to collector distance and 20 kv voltage and 0.1 ml flow rate were selected as optimized condition (**Figures.3 D and F**).

In the final step, CL was added to the solution of 10% PVA and electrospun under the optimized apparatus parameters. The SEM micrographs were taken from fabricated CL-loaded NFs and the pristine NFs. Continuous non-woven NFs with no beads or any phase separation and also smooth surface could be seen in the SEM micrographs of both pristine and CL-incorporated NFs. The mean diameter size of the optimized pristine PVA NFs and CL-loaded PVA NFs were calculated by Image J software from SEM micrographs. The mean diameter size for pristine NFs was 194.95±35.48 nm and 220.47±16.87 nm for CL-loaded NFs.

The reported thinner size calculated from SEM compared with the same value reported from AFM analyses is related to an overnight presence of NFs in the vacuum oven at room temperature before starting SEM analysis. This intervention evaporated any residual solvent that was still entrapped in the construction of the mats (**Figures. 4. A and B**). The incorporation of drug into the NFs did not

significantly change the NFs diameter sizes ($p>0.05$). Thus this fact and the observed smooth surface of fibers indicated that the CL loaded within the fibers (14).

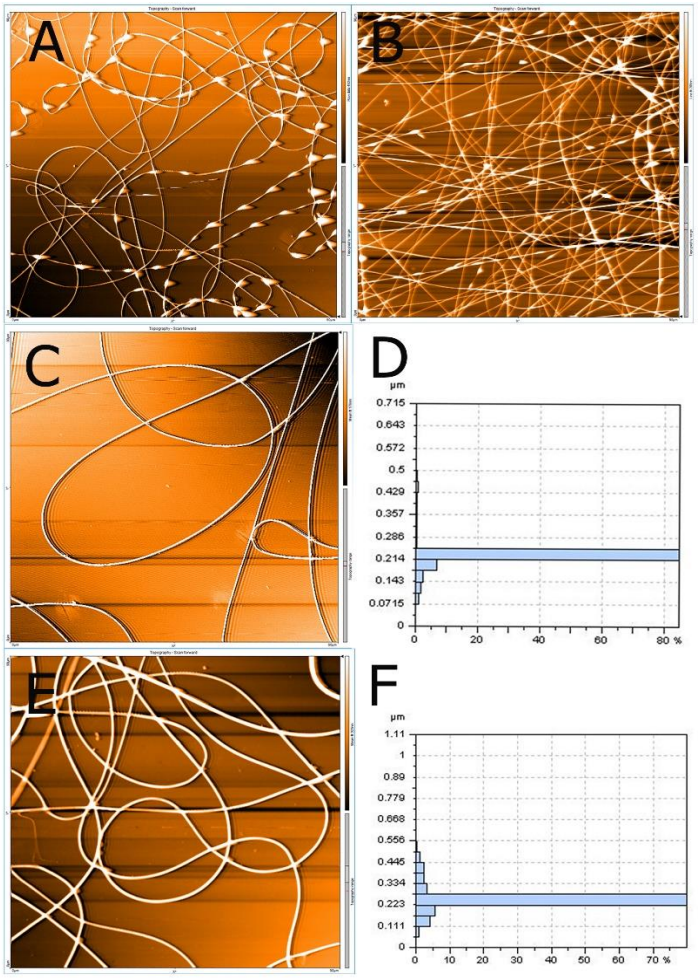

Fig.3: AFM micrographs of PVA 8% at 10cm, 20kv (A), and 20cm, 18kv (B), PVA 10% at 20cm, 20kv (C) with its size distribution (D), PVA 12% at 20cm, 20kv (E) with its size distribution (F).

In the final step, CL was added to the solution of 10% PVA and electrospun under the optimized apparatus parameters. The SEM micrographs were taken from fabricated CL-loaded NFs and the pristine NFs. Continuous non-woven NFs with no beads or any phase separation and also smooth surface could be seen in the SEM micrographs of both pristine and CL-incorporated NFs. The mean diameter size of the optimized pristine PVA NFs and CL-loaded PVA NFs were calculated by Image J software from SEM micrographs. The mean diameter size for pristine NFs was 194.95±35.48 nm and 220.47±16.87 nm for CL-loaded NFs. The reported thinner size calculated from SEM compared with the same value reported from AFM analyses is related to an overnight presence of NFs in the vacuum oven at room temperature before starting SEM analysis. This intervention evaporated any residual solvent that was still entrapped in the construction of the mats (**Figures. 4. A and B**). The incorporation of drug into the NFs did not significantly change the NFs diameter sizes ($p>0.05$). Thus this fact and the observed smooth surface of fibers indicated that the CL loaded within the fibers (14).

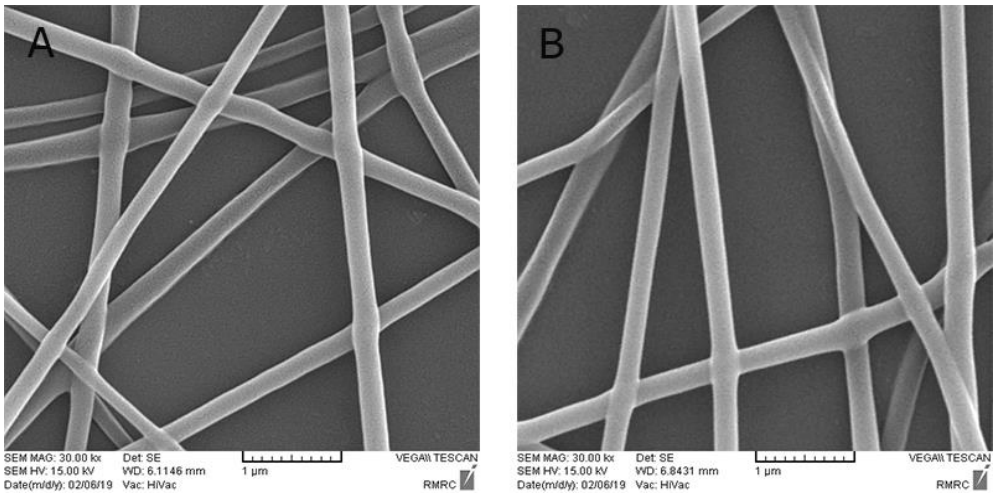

Fig. 4: SEM micrographs of PVA NFs (A) and CL-loaded PVA NFs (B).

3-2. FTIR molecular analysis

According to **Figure.5**, the FTIR spectrum of pure PVA showed main bands at 3450 cm^{-1} (O-H, stretching), 2921 (C-H of alkyls, stretching), 1652 (C=O, stretching) and 1101 (C-O, stretching) (15–18). The CL spectrum illustrated two peaks at 3315 and 3429 cm^{-1} which stand for O-H and N-H stretching. In the CL-loaded PVA NFs, the mentioned two peaks were combined and presented an individual peak which shows more intensity compared with the same band in PVA. This phenomenon determines the hydrogen bond formation between CL, which possesses poly oxygen structure, and the polymer's hydroxyl groups. Besides, the C-H stretching band of drug at 2935 cm^{-1} presented in the CL-loaded PVA NFs spectrum. Moreover, other characteristic peaks of CL, like 1733 (C=O, stretching), 1653 (C=O of amide, stretching), 1559 (N-H, bending), 1253 (C-O of ether, stretching), remained in the CL-loaded NFs spectrum with reduced intensity, which proves that the nitrogen and oxygen atoms of the drug participate in hydrogen bonding. No significant change of CL observed peaks in the drug loaded NFs spectrum might be related to homogeneous incorporation of CL through the polymeric NFs (19).

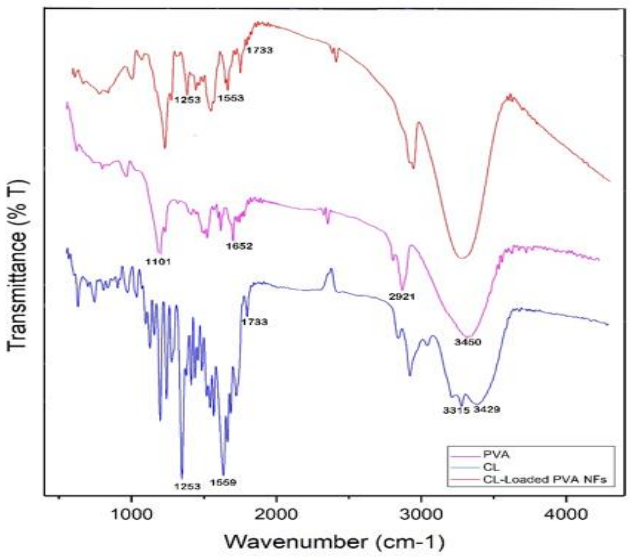

Fig.5: FT-IR spectra of pure powder of PVA, CL and the attained mat of CL-loaded PVA NFs.

3-3. STA Analysis

As illustrated in **Figure.6**, the DTA thermogram of pure PVA presented an endothermic peak at 81 ℃ which shows glass transition temperature (Tg). Two endothermic peaks at 222 ℃ and 297 ℃ are obvious that refers to melting and decomposition of the polymer. The remaining peaks determine the degradation steps of PVA planes (15, 17). The weight loss phases in TGA curve in three steps confirms the explained thermal behaviors. The DTA thermogram of PVA NFs in comparison with PVA powders demonstrates the omission of degradation peaks. Only the first three peaks were remained. This phenomenon refers to crystallinity reduction occurred by electrospinning process. Nevertheless, the weight loss phases are still visible in the TGA curve, proving all mentioned thermal behaviors (16).

The characteristic peak of pure CL with endothermic behavior at 160 ℃ which refers to melting point, completely vanished in CL-loaded PVA NFs curve. This fact determines the amorphous manner of CL in the NFs. The reported FT-IR results in this paper confirms this phenomenon. The DTA thermogram of CL-loaded PVA NFs, compared with PVA NFs, demonstrates the three characteristic peaks of PVA with a little shift. Two new peaks also manifested at higher temperatures that demonstrates higher crystallinity and enhanced thermal stability by CL incorporation. The TGA curve also shows a slight increase in the temperature of mass loss, which endorses the thermal stability enhancement. The reported increase in thermal stability could be explained by new hydrogen bond formation between CL and PVA functional groups that were proved by FT-IR analysis in part 4.2. Overall, the three phase TGA weight loss and the characteristic DTA peaks are similar in pristine PVA NFs and CL-loaded PVA NFs, confirming homogeneous distribution of CL through the PVA NFs in amorphous manner (16, 20). The amorphous manner of drug as one of the influential factors could provide better absorption and internalization of CL in the suggested formulation for topical, transdermal and transmucosal drug delivery systems (21).

3-4. Water angle analysis

The calculated water angle of PVA mats was 43.69±4.8°, however, the water droplet did not produce any angle with the CL-loaded PVA mats (**Figures. 7 A and B** as representative). The 0° water angle of the CL-loaded formulation could be observed in the video which is available in supplementary data. The loading of CL into the PVA NFs significantly reduced the contact angle and intensively increased the wettability of the mat. The observed wettability relates to enhance in NFs hydrophilicity due to homogenous distribution of hydrophilic drug.

The unique structure of CL which is surrounded by poly oxygen groups created the opportunity to form multiple hydrogen bindings with hydroxyl groups of PVA among all the NFs. Moreover, the NFs bear high surface area to volume that provides rapid and easy penetration of water molecules into the NFs mat. These observations in water angle values are in accordance with reported results in FT-IR and STA evaluations in the current study and also other previous papers (15, 22).

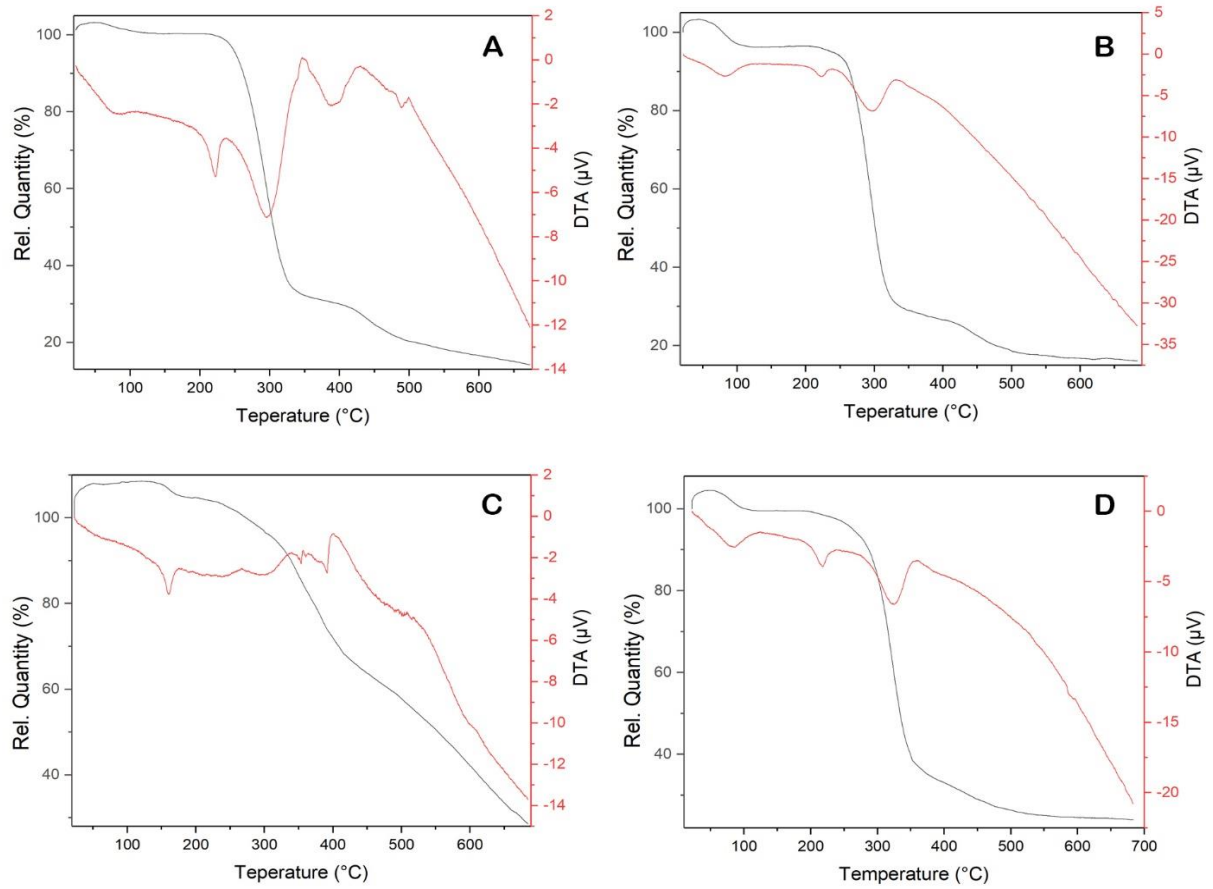

Fig.6: TGA, black curves and DTA, red curves of pure powder of PVA (A), PVA-NFs (B), pure CL (C) and CL-loaded PVA NFs (D).

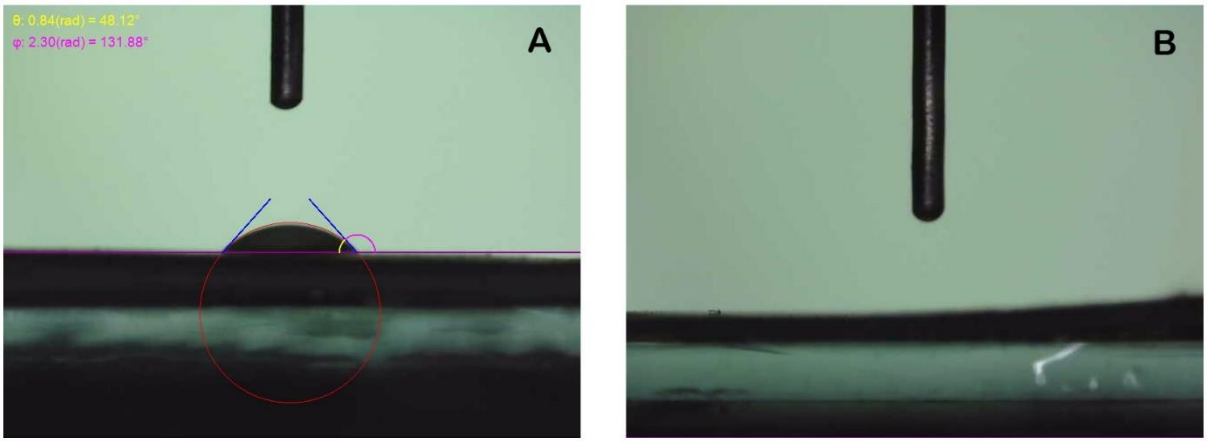

Fig.7: Representative water angles images of PVA NFs (A) and CL-loaded PVA NFs (B).

3-5. In vitro release profile

The high hydrophilicity of CL-loaded PVA NFs led us to carefully investigate the release profile of CL-NFs mat pieces in very short time intervals including 30, 60, 120, 240 and 360 seconds. The observed release profile demonstrated an immediate release of CL into the medium (**Figure.8**). As soon as the mat was exposed to the PBS medium, total loaded drug was released in less than 30 seconds. The rapid disappearance of CL-loaded PVA NFs in the dissolution medium refers to the approved high hydrophilicity that was reported in previous sections of the current study. In a recent study the solubility time of PVA, 10% w/v NFs were reduced to 5 seconds by adding 3% (w/w) emulsifying agent and also 1% (w/w) Tween-20 (23). The attained results from this study could suggest the achieved nanofiber based formulation as a novel and efficient fast dissolving Nano drug delivery system of CL.

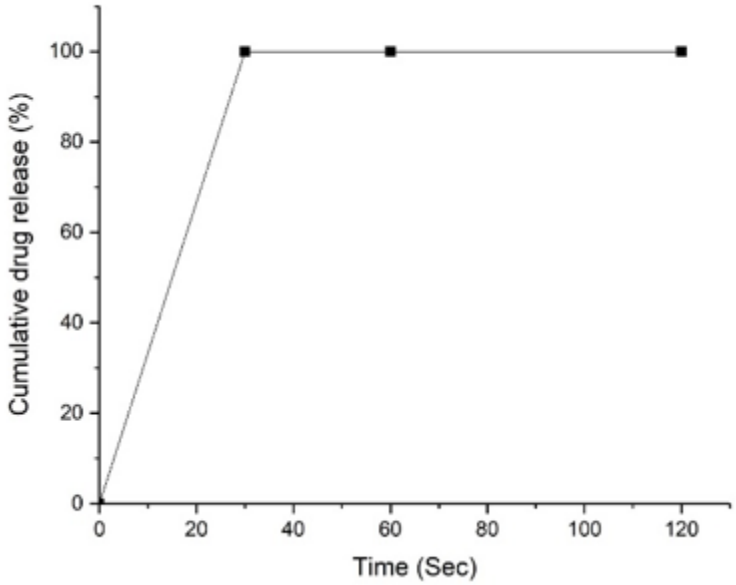

Fig.8: Rapid release profile of CL from CL-loaded PVA NF.

4- CONCLUSION

The NF based fast dissolving Nano drug delivery system of CL was formulated, optimized, and characterized. The optimized colchicine loaded NFs of PVA 10%w/v possesses 220.47±16.87 nm mean diameter size with smooth surface and obvious consistency. The drug and polymer were compatible and the thermal stability enhancement was reported by colchicine loading. The attained mat demonstrated a super hydrophilicity property and the in vitro release profile exhibited a rapid release of colchicine in 30 seconds. Thus the attained formulation could be suggested as a novel fast dissolving dosage form of CL for efficient management of its approved topical indications including, aphthous stomatitis, condylomata acuminata, psoriasis, actinic keratosis, etc., in pediatrics. It could also be suggested as a topical and systemic transmucosal drug delivery system through buccal cavity, sublingual space, nasal canal, vagina, rectum, ocular medium, etc., for systemic delivery of CL to bypass the first pass effect and enhance drug bioavailability. Thus, it could bring more convenience and compliance for pediatric patients. This technique could provide better management of hyperuricemia,

Familial Mediterranean fever and amyloidosis with lower administration doses that may reduce the risk of systemic toxicity. Moreover, considering the antitumor activity of CL may suggest it as a neoadjuvant or adjuvant chemotherapy formulation for management of topical tumor tissues.

5- CONFLICT OF INTEREST: None.

6- REFERENCES

1. Mano F, Martins M, Sá-Nogueira I, Barreiros S, Borges JP, Reis RL, et al. Production of Electrospun Fast-Dissolving Drug Delivery Systems with Therapeutic Eutectic Systems Encapsulated in Gelatin. AAPS PharmSciTech. 2017 Oct;18(7):2579–85.

2. Farkas B, Balogh A, Farkas A, Domokos A, Borbás E, Marosi G NZ. Medicated Straws Based on Electrospun Solid Dispersions. Polytech Chem Eng [Internet]. 2018;62(3):310-6.

3. Pimparade MB, Vo A, Maurya AS, Bae J, Morott JT, Feng X, et al. Development and evaluation of an oral fast disintegrating anti-allergic film using hot-melt extrusion technology. Eur J Pharm Biopharm Off J Arbeitsgemeinschaft fur Pharm Verfahrenstechnik eV. 2017 Oct;119:81–90.

4. Ben Halima N. Poly(vinyl alcohol): review of its promising applications and insights into biodegradation. RSC Adv [Internet]. 2016;6(46):39823–32. Available at: http://dx.doi.org/10.1039/C6RA05742J.

5. Nasiri F, Ajeli S, Semnani D, Jahanshahi M, Morad H. Fuzzy VIKOR Optimization for Designing High Performance Hydroxyapatite/Polycaprolactone Scaffolds for Hard Tissue Engineering. J Text Polym [Internet]. 2020;8(1):17–36. Available at: http://www.itast.ir/article_101562.html.

6. Thakkar S, Misra M. Electrospun polymeric nanofibers: New horizons in drug delivery. Eur J Pharm Sci. 2017 Sep;107:148–67.

7. Aytac Z, Yildiz ZI, Kayaci-Senirmak F, Tekinay T, Uyar T. Electrospinning of cyclodextrin/linalool-inclusion complex nanofibers: Fast-dissolving nanofibrous web with prolonged release and antibacterial activity. Food Chem. 2017 Sep;231:192–201.

8. Enayati-Fard R, Akbari J, Saeedi M, Morteza-Semnani K, Morad H, Nokhodchi A. Preparation and characterization of atenolol microparticles developed by emulsification and solvent evaporation. Lat Am J Pharm. 2019;38(7):1342-9.

9. Dubey KK, Kumar P, Labrou NE, Shukla P. Biotherapeutic potential and mechanisms of action of colchicine. Crit Rev Biotechnol. 2017 Dec;37(8):1038–47.

10. Goyal R, Macri LK, Kaplan HM, Kohn J. Nanoparticles and nanofibers for topical drug delivery. J Control Release. 2016 Oct;240:77–92.

11. Wang X, Ding B, Li B. Biomimetic electrospun nanofibrous structures for tissue engineering. Mater Today [Internet]. 2013;16(6):229–41. Available at: http://www.sciencedirect.com/science/article/pii/S136970211300196X.

12. Rockville M. United States Pharmacopeia and National Formulary (USP 41-NF 36). 41st-NF 36th ed. 2018. 1069–1070 p.

13. Sargazi G, Afzali D, Mostafavi A, Ebrahimipour SY. Synthesis of CS/PVA Biodegradable Composite Nanofibers as a Microporous Material with Well Controllable Procedure Through Electrospinning. J Polym Environ [Internet]. 2018;26(5):1804–17. Available at: http://dx.doi.org/10.1007/s10924-017-1080-8.

14. Elkasaby M, Hegab HA, Mohany A, Rizvi GM. Modeling and optimization of electrospinning of polyvinyl alcohol (PVA). Adv Polym Technol [Internet]. 2018 Oct 1;37(6):2114–22. Available at: https://doi.org/10.1002/adv.21869.

15. Torkamani AE, Syahariza ZA, Norziah MH, Wan AKM, Juliano P. Encapsulation of polyphenolic antioxidants obtained from Momordica charantia fruit within zein/gelatin shell core fibers via coaxial electrospinning. Food Biosci [Internet]. 2018;21:60–71. Available at: http://www.sciencedirect.com/science/article/pii/S2212429217306429.

16. Yang, S., Lei, P., Shan, Y., & Zhang D. Preparation and characterization of antibacterial electrospun chitosan/poly (vinyl alcohol)/graphene oxide composite nanofibrous membrane. Appl Surf SCINCE. 2018;435:832–40.

17. Alavarse AC, de Oliveira Silva FW, Colque JT, da Silva VM, Prieto T, Venancio EC, et al. Tetracycline hydrochloride-loaded electrospun nanofibers mats based on PVA and chitosan for wound dressing. Mater Sci Eng C Mater Biol Appl. 2017 Aug;77:271–81.

18. Mei. Yang, Runjun. Sun, Yan. Feng, Honghong. Wang HD and CL. Preparation, characterization and kinetics study of chitosan/PVA electrospun nanofiber membranes for the adsorption of dye from water [Internet]. Vol. 39, Journal of Polymer Engineering. 2019. p. 459. Available at: https://www.degruyter.com/view/j/polyeng.2019.39.issue-5/polyeng-2018-0275/polyeng-2018-0275.xml.

19. Ahmed R, Tariq M, Ali I, Asghar R, Noorunnisa Khanam P, Augustine R, et al. Novel electrospun chitosan/polyvinyl alcohol/zinc oxide nanofibrous mats with antibacterial and antioxidant properties for diabetic wound healing. Int J Biol Macromol. 2018 Dec;120(Pt A):385–93.

20. Siddiqui SA Dwivedi A, Pandey A, Singh PK, Hasan T, Jain S, et al. Molecular Structure, Vibrational Spectra and Potential Energy Distribution of Colchicine Using <I>ab Initio</I> and Density Functional Theory. J Comput Chem Japan. 2009;8(2):59–72.

21. Hadinejad F, Jahanshahi M, Morad H. Microwave-assisted and ultrasonic phyto-synthesis of copper nanoparticles; A comparison study. Nano Biomed Eng. 2021;13 (1): 6-20

22. Park JH, Lee HW, Chae DK, Oh W, Yun JD, Deng Y, et al. Electrospinning and characterization of poly(vinyl alcohol)/chitosan oligosaccharide/clay nanocomposite nanofibers in aqueous solutions. Vol. v. 287, Colloid & polymer science. Berlin/Heidelberg : Springer-Verlag; 2009.

23. Rezaeinia H, Emadzadeh B, Ghorani B. Electrospun balangu (Lallemantia royleana) hydrocolloid nanofiber mat as a fast-dissolving carrier for bergamot essential oil. Food Hydrocoll [Internet]. 2020;100:105312. Available at: http://www.sciencedirect.com/science/article/pii/S0268005X19314110.